ACS APPLIED MATERIALS & INTERFACES

RESEARCH ARTICLE

www.acsami.org

Hepta(3,3,3-trifluoropropyl) Polyhedral Oligomeric Silsesquioxane-capped Poly(*N*-isopropylacrylamide) Telechelics: Synthesis and Behavior of Physical Hydrogels

Lei Wang, Ke Zeng, and Sixun Zheng*

Department of Polymer Science and Engineering and State Key Laboratory of Metal Matrix Composites, Shanghai Jiao Tong University, Shanghai 200240, P. R. China

ABSTRACT: Hepta(3,3,3-trifluoropropyl) polyhedral oligomeric silsesquioxane (POSS)-capped poly(N-isopropylacrylamide) (PNIPAAm) telechelics with variable lengths of PNIPAAm midblocks were synthesized by the combination of reversible addition−fragmentation chain transfer polymerization (RAFT) and the copper-catalyzed Huisgen 1,3-cycloaddition (i.e., click chemistry). The POSS-capped trithiocarbonate was synthesized and used as the chain transfer agent for the RAFT polymerization of N-isopropylacrylamide. The organic−inorganic amphiphilic telechelics were characterized by means of nuclear magnetic resonance spectroscopy (NMR) and gel permeation chromatography (GPC). Atomic force microscopy (AFM) shows that all the POSS-capped PNIPAAm telechelics exhibited microphase-separated morphologies, in which the POSS terminal groups were self-assembled into the microdomains and dispersed into the continuous PNIPAAm matrices. The POSS nanodomains could behave as the physical cross-linking sites and as a result the physical hydrogels were formed while these POSS-capped PNIPAAm telechelics were subjected to the solubility tests with water. These physical hydrogels possessed well-defined volume phase transition phenomena and displayed rapid reswelling and deswelling thermoresponsive behavior compared to control PNIPAAm hydrogel.

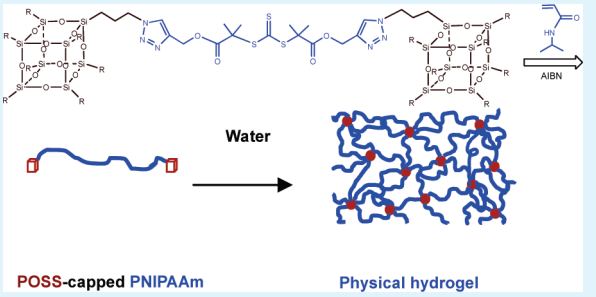

KEYWORDS: polyhedral oligomeric silsesquioxane, poly(N-isopropylacrylamide), telechelics and physical hydrogels

INTRODUCTION

Polyhedral oligomeric silsesquioxane (POSS) reagents, monomers, and polymers are emerging as a new chemical technology for preparing the organic−inorganic hybrids.[1−3] During the past decade, POSS-containing organic−inorganic hybrids have become the focus of many studies because of the excellent comprehensive properties of this class of hybrid materials, such as mechanical properties, thermal stability and flame retardation etc.[1−3] Recently, it has been identified that POSS could be employed to optimize the properties of some functional materials via the formation of specific morphological structures.[4−24]

Stimuli-responsive hydrogels have attracted considerable interests owing to their ability to change volume or shape in response to environmental alteration. The environment-responsive properties have potential applications in biomedical and biochemical fields such as drug delivery and protein separation.[25−28] Poly(*N*-alkylacrylamide) hydrogels are among the most-investigated hydrogel systems during the past decades.[29−35] Of them, poly(*N*-isopropylacrylamide) (PNIPAAm) hydrogels can exhibit a volume phase transition (VPT) behavior as the environmental temperature changes,[29−31,36] which stems from the lower critical solution temperature (LCST) behavior of PNIPAAm chains in aqueous solution.[37−41] However, PNIPAAm hydrogels inherently displayed slow deswelling and reswelling rates due to the collective diffusion of water molecules in the cross-linked networks.[42−46] Therefore, the modification of PNIPAAm hydrogels is necessary to meet the requirement of application of the hydrogels. Recently, there have been several reports on the modification of PNIPAAm hydrogels with POSS macromers.[7−10] Schiraldi et al.[7] ever used octamethacryloxylpropyl POSS as a cross-linking agent of PNIPAAm to promote the interactions between the cross-linking agent and silicate filler in the clay-containing poly(*N*-isopropylacrylamide) hydrogels. Mu et al.[8] have reported the modification of PNIPAAm hydrogels via in situ cross-linking with an octafunctional POSS macromer and it was found that the thermoresponsive properties of PNIPAAm hydrogels were significantly improved compared to the control PNIPAAm hydrogel. More recently, Zeng et al.[9] prepared the organic−inorganic PNIPAAm hydrogels via the copolymerization of NIPAAm with 3-acryloxypropylhepta(3,3,3-trifluoropropyl) POSS and found that the POSS-containing PNIPAAm hydrogels displayed much faster temperature response rates than plain PNIPAM hydrogel.

POSS-capped telechelic polymers are a class of interesting organic−inorganic hybrids owing to their specific topologies and self-assembly behaviavor.[10,16−24,47−50] Mather et al.[47] first reported the synthesis of heptacyclohexyl POSS-capped poy(ethylene oxide) (PEO) telechelics via the direct reaction of isocyanatopropyldimethylsilylheptacyclohexyl POSS with poly(ethylene

Received: December 21, 2010
Accepted: February 18, 2011
Published: March 07, 2011

glycol) (PEG) and the behavior of crystallization and rehology was invesitgated.[48,49] Zeng et al.[10] synthesized hepta(3,3,3-trifluoropropyl) POSS-capped PEO telechelics via copper-catalyzed Huisgen cycloaddition reaction (i.e., click chemistry) between 3-azidopropylhepta(3,3,3-trifluoropropyl) POSS and alkyne-terminated PEO. More recently, Mueller et al.[50] reported the synthesis of POSS-capped polystyrene telechelics via the combination of atom transfer radical polymerization (ATRP) and the copper-catalyzed Huisgen 1,3-cycloaddition. All these POSS-capped telechelic polymers were obtained via the reaction of the end groups of existing polymers with POSS, i.e., the so-called "POSS-terminating" approach was employed; this approach is effective for the preparation of the POSS-capped telechelic polymers with relatively low molecular weights. Nonetheless, the efficiency of this route is open to question for the preparation of high-molecular-weight samples because it is not easy to ensure that all the ends of the polymers are capped with POSS because of too low concentration of end groups. To the best of our knowledge, however, there have been no precedent reports on the POSS-capped PNIPAAm telechelics.

In this contribution, we report a synthesis of POSS-capped PNIPAAm telechelics with a "POSS-spreading" strategy. In this approach, a POSS-capped trithiocarbonate was synthesized and used as a chain transfer agent, with which the reversible addition−fragmentation chain transfer polymerization (RAFT) of NIPAAm was carried out. With the insertion of NIPAAm, the two POSS end groups were spread and the POSS-capped PNIPAAm telechelics with variable length of PNIPAAm were afforded. With this approach, the ends of PNIPAAm chains were capped with two hepta(3,3,3-trifluoropropyl) POSS groups, which are quite hydrophobic.[9,10,51,52] The POSS-capped PNIPAAm telechelics could display some interesting properties owing to the combination of the thermoresponsive midblock (viz. PNIPAAm) and bulky and hydrophilic end groups (viz. POSS). It is expected that the microphase-separated morphology in bulk could be exhibited in the organic−inorganic telechelic polymers because of the immiscibility between PNIPAAm and the POSS, in which the POSS microdomains are dispersed in continuous PNIPAAm matrix. In water, the POSS microdomains could behave as physically cross-linking sites and thus the PNIPAAm physical hydrogels could be afforded. In this work, the POSS-capped PNIPAAm telechelics were characterized by means of nuclear magnetic resonance spectroscopy (NMR) and gel permeation chromatography (GPC). The morphology and surface properties of the organic−inorganic telechelics were investigated by means of atomic force microscopy (AFM) and static contact angle analysis. The thermoresponsive behavior of the physical hydrogels was addressed on the basis of swelling, deswelling, and reswelling tests.

EXPERIMENTAL SECTION

Materials. 3,3,3-Trifluoropropyltrimethoxysilane (99%) was obtained from Zhejiang Chem-Technology Co., China. 3-Bromopropyltrichlorosilane ($BrCH_2CH_2CH_2SiCl_3$), sodium azide (NaN_3) and pentamethyldiethylene triamine (PMDETA) were purchased from Aldrich Co, USA and used as received. *N*-Isopropylacrylamide (NIPAAm) was prepared in this lab by following the literature method.[53] Propargyl alcohol (98%) was purchased from Aladdin Reagent Co., Shanghai, China. Other reagents such as metal sodium, calcium hydride (CaH_2), sodium hydroxide (NaOH) 2,2-azobisisobutylnitrile (AIBN), thionyl chloride and carbon disulfide (CS_2) were of chemically pure grade, purchased from Shanghai Reagent Co., China. The solvents such as *N*,*N*-dimethylformamide (DMF), tetrahydrofuran (THF), dichloromethane, chloroform, acetone, pyridine, petroleum ether (distillation range: 60−90 °C), and triethylamine (TEA) were of chemically pure grade, also obtained from commercial sources. Before use, THF was refluxed above sodium and then distilled and stored in the presence of the molecular sieve of 4 Å. TEA was refluxed over CaH_2 and then was treated with *p*-toluenesulfonyl chloride, followed by distillation.

Synthesis of 3-Bromopropylhepta(3,3,3-trifluoropropyl) POSS. Hepta(3,3,3-trifluoropropyl)tricycloheptasiloxane trisodium silanolate $[Na_3O_{12}Si_7(C_3H_4F_3)_7]$ was synthesized by following the method of literature reported by Fukuda et al.[54] In a typical experiment, (3,3,3-trifluoropropyl)trimethoxysilane $[CF_3CH_2CH_2Si(OMe)_3]$ (50.0 g, 0.23 mol), THF (250 mL), deionized water (5.25 g, 0.29 mol) and sodium hydroxide (3.95 g, 0.1 mol) were charged to a flask equipped with a condenser and a magnetic stirrer. After refluxed for 5 h, the reactive system was cooled down to room temperature and held at this temperature with vigorous stirring for additional 15 h. All the solvent and other volatile were removed via rotary evaporation and the white solids were obtained. After dried at 40 °C in vacuo for 12 h, 37.3 g products were obtained with the yield of 98%. 3-Bromopropylhepta(3,3,3-trifluoropropyl) POSS was prepared via the corner capping reaction between $Na_3O_{12}Si_7(C_3H_4F_3)_7$ and 3-bromopropyl trichlorosilane. Typically, $Na_3O_{12}Si_7(C_3H_4F_3)_7$ (10.0 g, 8.8 mmol) and triethylamine (1.3 mL, 8.8 mmol) were charged to a flask equipped with a magnetic stirrer, 200 mL anhydrous THF were added with vigorous stirring. The flask was immersed into an ice−water bath and purged with highly pure nitrogen for 1 h. After that, 3-bromopropyltrichlorosilane (2.47 g, 9.68 mmol) dissolved in 20 mL anhydrous THF were slowly dropped within 30 min. The reaction was carried out at 0 °C for 4 h and at room temperature for 20 h. The insoluable solids (i.e., sodium chloride) was filtered out and the solvent together with other volatile was removed via rotary evaporation to afford the white solids. The solids were washed with 50 mL methanol for three times and dried in vacuo at 40 °C for 24 h and 8.2 g of product was obtained with the yield of 76%. FTIR (cm^{-1}, KBr window): 1090−1000 (Si-O-Si), 2900−2850 (-CH_2), 1120−1300 (-CF_3), 540 (C-Br). ^{1}H NMR (ppm, acetone-d_6): 3.52 (*t*, 2.0H, -C**H**$_2$-Br), 2.32 (*m*, 14.0H, SiCH$_2$C**H**$_2$CF$_3$), 1.96 (*m*, 2.0H, -C**H**$_2$-CH$_2$-Br), 1.03 (*m*, 14.0H, SiC**H**$_2$CH$_2$CF$_3$), 0.96 (*t*, 2.0H, -C**H**$_2$-CH$_2$-CH$_2$-Br). ^{29}Si NMR (ppm, acetone-d_6): −65.8, −66.8, and −67.0. MALDI-TOF-MS (product + Na^+): 1240.1 Da.

Synthesis of 3-Azidopropylhepta(3,3,3-trifluoropropyl) POSS. 3-Azidopropylhepta(3,3,3-trifluoropropyl) POSS was synthesized via the reaction between 3-bromopropylhepta(3,3,3-trifluoropropyl) POSS and sodium azide (NaN_3). Typically, 3-bromopropylhepta(3,3,3-trifluoropropyl) POSS (3.0 g, 2.5 mmol) and NaN_3 (0.1760 g, 2.75 mmol) were charged to a flask equipped with a magnetic stirrer and 10 mL of anhydrous DMF was added to the flask. The reaction was carried out at the room temperature for 24 h. After that, a large amount of deionized water was used to perticipate the product. The products was further dried at 40 °C in a vacuum oven for 24 h. The product (2.6 g) was obtained with the yield of 90%. FTIR (cm^{-1}, KBr window): 1090−1000 (Si-O-Si), 2900−2850 (-CH_2), 1120−1300 (-CF_3), 2105 (azido). ^{1}H NMR (ppm, acetone-d_6): 3.35 (*t*, 2.0H, -C**H**$_2$-N$_3$), 2.32 (*m*, 14.0H, SiCH$_2$C**H**$_2$CF$_3$), 1.76 (*m*, 2.0H, -C**H**$_2$-CH$_2$-N$_3$), 1.03 (*m*, 14.0H, SiC**H**$_2$CH$_2$CF$_3$), 0.86 (*t*, 2.0H, -C**H**$_2$-CH$_2$-CH$_2$-N$_3$).

Synthesis of S,S′-Bis(α, α′-dimethyl-α″-propargyl acetate)-trithiocarbonate. S,S′-Bis(α,α′-dimethyl-α″-acetic acid)-trithiocarbonate (BDATC) was synthesized by following the method of literature.[55−58] Typically, carbon disulfide (6.85 g, 0.09 mol), chloroform (26.875 g, 0.225 mol), acetone (13.075 g, 0.225 mol), tetrabutylammonium bromide (0.572 g, 1.775 mmol), and 30 mL of mineral spirits were charged into a three-necked flask equipped with a mechanical stirrer. The flask was immersed into an ice−water bath

and purged with highly pure nitrogen. Sodium hydroxide solution (50%) (50.5 g, 0.63 mol) were slowly dropped within 30 min. The reaction was carried out at room temperature overnight and then 225 mL water was then added to dissolve the solid, followed by adding 30 mL of concentrated HCl to acidify the aqueous layer. After vigorous stirring for additional 30 min, the earth-colored insoluable solids was filtered out and washed with water thrice. After being dried in vacuo at 40 °C for 24 h, the crude product was collected. The resulting product was obtained by recrystallization in the mixture of toluene with actone (4/1 v/v) to afford yellow crystalline solids. ^{1}H NMR (ppm, $CDCl_3$): 1.69 (*s*, -CSSC-($C\mathbf{H_3}$)$_2$COO). ^{13}C NMR (ppm, DMSO-d_6): 25.6 [-CSSC($\mathbf{C}H_3$)$_2$COO], 56.8 [-CSS$\mathbf{C}$(CH$_3$)$_2$COO], 173.7 [-CSSC(CH$_3$)$_2\mathbf{C}$OO], 219.8 [-$\mathbf{C}$SSC(CH$_3$)$_2$COO].

Synthesis of S, S′-Bis(α,α′-dimethyl-α′′-propargyl acetate)-trithiocarbonate. S,S′-Bis(α,α′-dimethyl-α′′-propargyl acetate)-trithiocarbonate was synthesized via the esterification of S,S′-bis(α, α′-dimethyl-α′′-acetic acid)-trithiocarbonate with propargyl alcohol.[59−62] First, 3.10 g of propargyl alcohol (27.60 mmol), 1 mL of pyridine, and 15 mL of dichloromethane were charged to a flask immersed into an ice−water bath. BDATC (0.78 g, 2.762 mmol) and thionyl chloride (20 mL $SOCl_2$) were charged to another flask with vigorous stirring for 3 h at 60 °C. After excess thionyl chloride ($SOCl_2$) was distilled out, 5 mL of anhydrous dichloromethane was added to system and the solution was dropwise added to the above flask containing propargyl alcohol. With continuous stirring for 24 h at room temperature, the reacted solution was washed free of propargyl alcohol and pyridine chloride by water and then dried over sodium sulfate. The solvent, dichloromethane, was removed via rotary evaporation to afford 0.85 g alkyne-capped trithiocarbonates with the yield of 86%. ^{1}H NMR (ppm, $CDCl_3$): 1.67 (*s*, 6.0H, -CSSC-($C\mathbf{H_3}$)$_2$COOCH$_2$CCH), 2.46 (*t*, 1.0H, -CSSC(CH$_3$)$_2$COOCH$_2$CC$\mathbf{H}$), 4.67 (*d*, 2.0H, -CSSC(CH$_3$)$_2$COO$\mathbf{CH_2}$CCH).

Synthesis of POSS-capped Trithiocarbonate. The above alkyne-capped trithiocarbonate (BDPT) was used to reacted with the 3-azidopropylhepta(3,3,3-trifluoropropyl) POSS to afford the POSS-capped trithiocarbonate. Typically, BDPT (0.1 g, 0.279 mmol) and 3-azidopropylhepta (3,3,3-trifluoropropyl) POSS (0.658 g, 0.558 mmol) were added to a 25 mL flask equipped with a magnetic stirrer and 6 mL THF was charged. The system was purged with highly pure nitrogen for 40 min and then Cu(I)Br (4.0 mg) and PMDETA (5.7 μL) were added and the system was connected to a standard Schlenk line and degassed using three freeze−evacuate−thaw cycles. The reaction was carried out at room temperature for 24 h and the reacted solution was passed though a neutral aluminum oxide column to remove the copper catalyst with tetrahydrofuran as the eluent. The solution was concentrated via rotary evaporation and then precipitated in petroleum ether. The resulting product (0.621 g) was obtained with the yield of 82%. ^{1}H NMR (ppm, $CDCl_3$): 0.78 (*m*, 2.0H, SiC$\boldsymbol{H_2}$CH$_2$CH$_2$-trizole), 1.01 (*m*, 14.0H, SiC$\boldsymbol{H_2}$CH$_2$CF$_3$), 1.62 (*s*, 6.0H, -CSSC($C\mathbf{H_3}$)$_2$COOCH$_2$-trizole), 2.10 (*m*, 2.0H, SiCH$_2$C$\mathbf{H_2}$CH$_2$-trizole), 2.30 (*m*, 14.0H, SiCH$_2$C$\boldsymbol{H_2}$CF$_3$), 4.44 (*m*, 2.0H, SiCH$_2$CH$_2$C$\mathbf{H_2}$-trizole), 5.20 (*d*, 2.0H, -CSSC-(CH$_3$)$_2$COOC$\mathbf{H_2}$-trizole), 8.16 (*d*, 1.0H, protons of trizole).

Synthesis of POSS-capped Poly(*N*-isopropylacrylamide) Telechelics. The POSS-trithiocarbonate was used as the chain transfer agent (CTA) to obtain POSS-capped poly(N-isopropylacrylamide) telechelics via reversible addition−fragmentation chain transfer (RAFT) polymerization. Typically, to a 50 mL flask equipped a magnetic stirrer the CTA (0.167 g, 0.0615 mmol), N-isopropylacrylamide (NIPAAm) (1.23 g) and 1,4-dioxane (9.5 mL) were charged and 2,2-azobisisobutylnitrile (4.0 mg, 0.024 mmol) was used as the initiator. The flask was connected to a Shlenk line and three freeze−evacuate−thaw cycles were used to remove a trace of oxygen. The flask was immersed into an oil bath at 65 °C and the polymerization was carried out for 20 h. The crude polymer was dissolved in THF and the mixture was precipitated in excess petroleum ether. This procedure was repeated for three times to purify the products. After dried in a vacuum oven at 30 °C, 0.89 g of polymer was obtained with the conversion of NIPAAm monomer to be 75.0%. The molecular weight of the block copolymer was determined by means of gel permeation chromatography (GPC) to be M_n =15 900 with M_w/M_n =1.72.

Preparation of Control PNIPAAm Network. N-isopropylacrylamide (2.0 g) and N,N′-methylenebisacrylamide (27.3 mg) were charged to a glass tube and anhydrous 1,4-dioxane (2 mL) was added. The system was purged with highly pure nitrogen for 30 min, and 4 mg AIBN was added. The radical polymerization was initiated and performed at 60 °C for 24 h. With the polymerization proceeding, the system was gradually gelled. The gel was respectively extracted with water and THF for 72 h for remove unreated NIPAAm. The gel was dried in vacuo at 60 °C for 48 h.

Techniques and Measurement. *Nuclear Magnetic Resonance Spectroscopy (NMR).* The ^{1}H NMR measurements were carried out on a Varian Mercury Plus 400 MHz NMR spectrometer. The samples were dissolved with deuterium acetone (acetone-d_6) or chloroform ($CDCl_3$) and the solutions were measured with tetramethylsilane (TMS) as the internal reference. The ^{29}Si NMR spectra were obtained using a Bruker Avance III 400 MHz NMR spectrometer.

Gel Permeation Chromatography (GPC). The molecular weights were measured by gel permeation chromatography (GPC) on a Perkin-Elmer Series 200 system (100 μL injection column, 10 μm PL gel 300 mm × 7.5 mm mixed B columns) equipped with a RI detector. N,N′-dimethylformamide (DMF) containing 0.01 mol/L lithium bromide was used as eluent at a flow rate of 1.0 mL/min. The column system was calibrated by standard polystyrene.

Atomic Force Microscopy (AFM). The specimens for AFM measurement were prepared via spin-coating the solution of the POSS-capped PNIPAAm on cleaned glass slides. The POSS-capped PNIPAAm telechelic polymers were dissolved in THF to prepare the solution with the concentration of 10 wt %; the solution was spin-coated at the speed of 1800 r/min on cleaned glass slides to form a flat and thin layer. The specimens were further dried and annealed in vacuo at 80 °C for 3 h prior to the measurment and the thickness of films was estimated to be 20 μm. The AFM experiments were performed with a Nanoscope IIIa scanning probe microscope (Digital Instruments, Santa Barbara, CA). Tapping mode was employed in air using a tip fabricated from silicon (125 μm in length with ca. 500 kHz resonant frequency). Typical scan speeds during recording were 0.3−1 lines s^{-1} using scan heads with a maximum range of 5 μm × 5 μm.

Determination of Cloud Points. Typically, the POSS-capped PNIPAAm telechelics (0.01 g) were dissolved in 0.5 mL of THF and then 50 mL of ultrapure water was added dropwise by a dropping funnel with vigorous stirring. After additional stirring for 30 min, a transparent emulsion was formed with the concentration of the polymer being 0.02 wt % and the THF was eliminated via rotary evaporation. The cloud points were determined with a Perkin-Elmer Lambda 20 Ultraviolet−visible spectrometer at the wavelength of light to be λ = 550 nm. A thermostatically controlled couvette was employed and the plots of light transmittance as a function of temperature were obtained at the heating rate of 0.5 °C/min.

Surface Contact Angle Analysis. The specimens for surface contact angle analysis were identical with those for AFM measurements. The static contact angle measurements with ultrapure water were carried out on a KH-01−2 contact angle measurement instrument (Beijing Kangsente Scinetific Instruments Co., China) at room temperature. For variable-temperature measurements, the specimens were held at specific temperature for 10 min before the measurements.

Swelling, Deswelling, and Reswelling Kinetics. The POSS-capped PNIPAAm samples were charged to glass tubes with the diameter of 10 mm and a small amount of tetrahydrofuran was added to dissolve the samples. The solvent was slowly evaporated at room temperature for 2 days and the residual solvent was eliminated *in vacuo* at 40 °C overnight.

Scheme 1. Synthesis of 3-Azidopropylhepta(3,3,3-trifluoropropyl) POSS

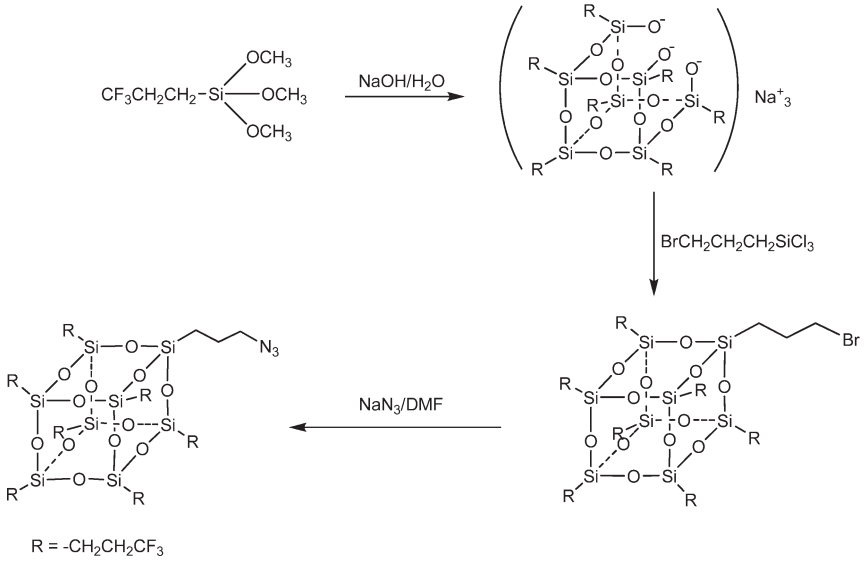

The specimens for swelling, deswelling and reswelling tests were cut from the dried cylindered samples with the identical diameter and the heights of specimens were controlled to be *c.a.* 3 mm. Swelling ratios of hydrogels were gravimetrically measured after wiping off the water on the surface with moistened filter paper in the temperature range from 22 to 48 °C. All of the gel samples were dipped in distilled water for at least 24 h at every particular temperature. Swelling ratio is defined as follows:

$$\text{swelling ratio} = W_s/W_d \quad (2)$$

where W_s is the weight of the water in the swollen gel at a particular temperature and W_d is the weight of the as-dried gel.

The deswelling kinetics of hydrogels was gravimetrically measured at 48 °C after wiping off water on the surface with moistened filter paper. Prior to the measurement, the gel samples were equilibrated in distilled water at room temperature (25 °C) for 24 h. The weight changes of gels were recorded with regular time intervals. Water retention is defined as follows

$$\text{water retention} = (W_t - W_d)/W_s \times 100\% \quad (3)$$

where W_t is the weight of the gel at regular time intervals and the other symbols are the same as defined above.

The kinetics of reswelling of hydrogels was gravimetrically measured at 22 °C. The reswelling kinetics of gels was measured at the equilibrium in distilled water at 48 °C for 24 h. After water was wiped off the surface, the weight changes of gels were recorded at regular time intervals. Water uptake is defined as follows

$$\text{water uptake} = (W_t - W_d)/W_s \times 100\% \quad (4)$$

where W_t is the weight of the gels at regular time intervals and the other symbols are the same as defined above.

RESULTS AND DISCUSSION

Synthesis of POSS-capped PNIPAAm Telechelics. The route of synthesis for the POSS-capped PNIPAAm telechelics was outlined in Schemes 1 and 2. To afford the POSS-capped PNIPAAm telechelics, the reversible addition−fragmentation chain transfer (RAFT) polymerization of NIPAAm was carried out with a POSS-capped trithiocarbonate as the chain transfer agent. The POSS-capped trithiocarbonate was obtained *via* the copper-catalyzed Huisgen 1,3-cycloaddition reaction between S,S′-bis(α, α′-dimethyl-α″-propargyl acetate) trithiocarbonate (BDPT)[55−58] and 3-azidopropylhepta (3,3,3-trifluoropropyl) POSS. BDPT was prepared via the esterification reaction of S,S-bis(α,α′-dimethyl-α″-acetic acid)-trithiocarbonate (BDAT) with propargyl alcohol, which was mediated by thionyl chloride and pyridine. Shown in Figure 1 are the ^{1}H NMR spectra of BDAT and BDPT. BDAT is characterized by the resonance of methyl protons at 1.70 ppm. With occurrence of the esterification, the resonance of the methyl protons slightly shifted to high field (viz. at 1.67 ppm). Concurrently, there appeared two new signals of resonance at 2.46 ppm and 4.67 ppm, which are assignable to the protons of alkyne and methylene groups connected to ester group, respectively. In view of the ratio of integral intensity of alkyne protons to that of methylene and methyl protons, it is judged that the esterification reaction has been carried out to completion and thus BDPT was successfully obtained. The preparation of 3-azidopropylhepta(3,3,3-trifluoropropyl) POSS has been previously reported[10] and herewith, the route of synthesis was outlined in brief. The starting compound for the POSS macromer is hepta(3,3,3-trifluoropropyl) tricycloheptasiloxane trisodium silanolate [$Na_3O_{12}Si_7(C_3H_4F_3)_7$], which was prepared via the condensation and arrangement of 3,3,3-trifluoropropyltrimethoxysilane in the presence of sodium hydroxide.[10] The corner-capping reaction between hepta-(3,3,3-trifluoropropyl) tricycloheptasiloxane trisodium silanolate and 3-bromopropyltrichlorosilane was utilized to obtain 3-bromopropylhepta(3,3,3-trifluoropropyl) POSS, which was further reacted with sodium azide (NaN_3) to afford 3-azidopropylhepta(3,3,3-trifluoropropyl) POSS. The results of ^{1}H, ^{13}C, and ^{29}Si NMR and MALDI-TOF-mass spectroscopy demonstrated that 3-azidopropylhepta(3,3,3-trifluoropropyl) POSS was successfully obtained.[10] The copper-catalyzed Huisgen 1,3-dipolar cycloaddition between the 3-azidopropylhepta(3,3,3-trifluoropropyl) POSS and BDPT was carried out to obtain the POSS-capped trithiocarbonate. As shown in Figure 1, the signal of resonance at 8.16 ppm was assignable to the protons of triazole structure, which is characteristic of the Huisgen 1,3-dipolar cycloaddition (i.e., so-called click reaction). The disappearance of the resonance at 2.46 ppm assignable to the

Scheme 2. Synthesis of POSS-capped PNIPAAm Telechelics

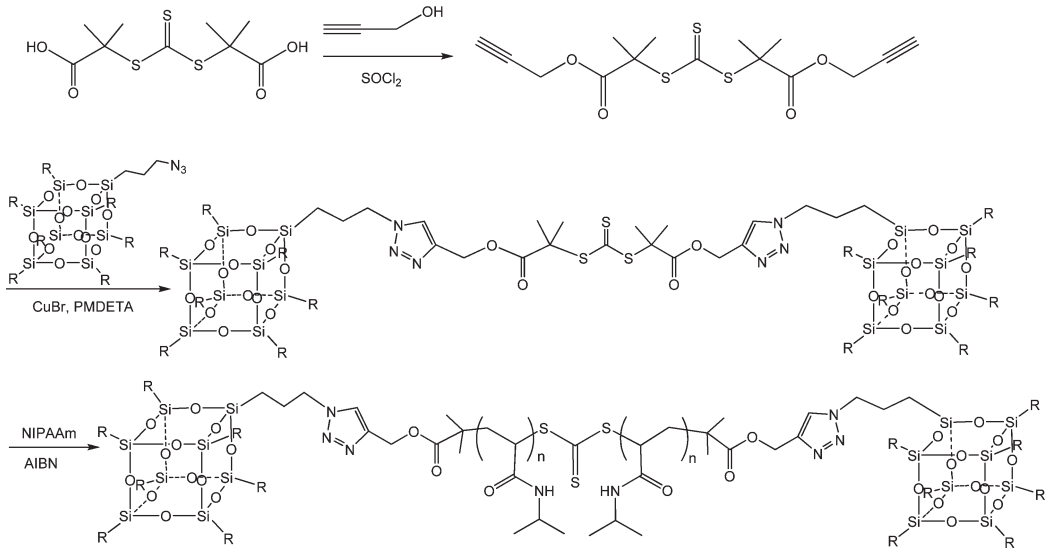

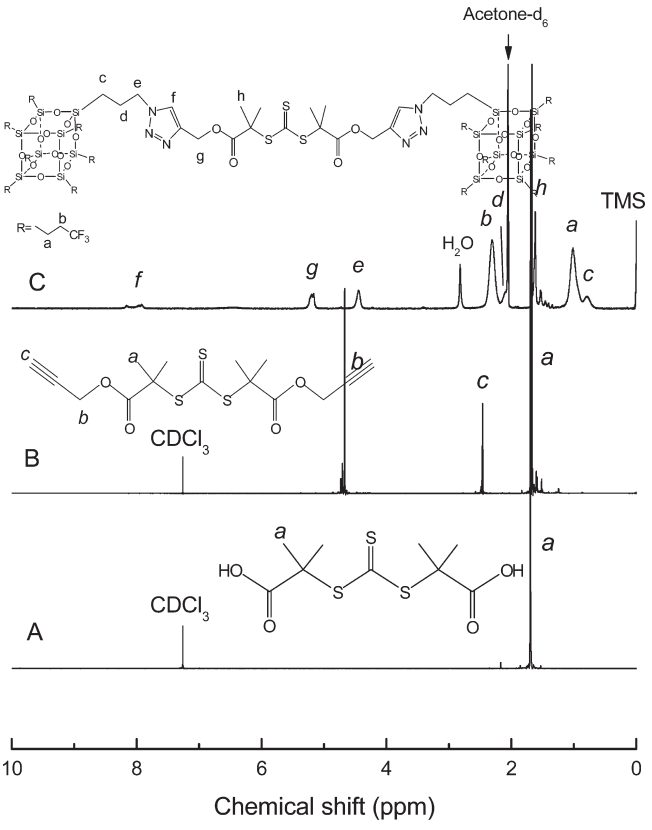

Figure 1. ^{1}H NMR spectra of: (A) S,S-bis(α,α′-dimethyl-α″-acetic acid)-trithiocarbonate (BDAT); (B) S,S′-bis(α,α′-dimethyl-α″-propargyl acetate) trithiocarbonate (BDPT); (C) POSS-capped thrithiocarbonate;.

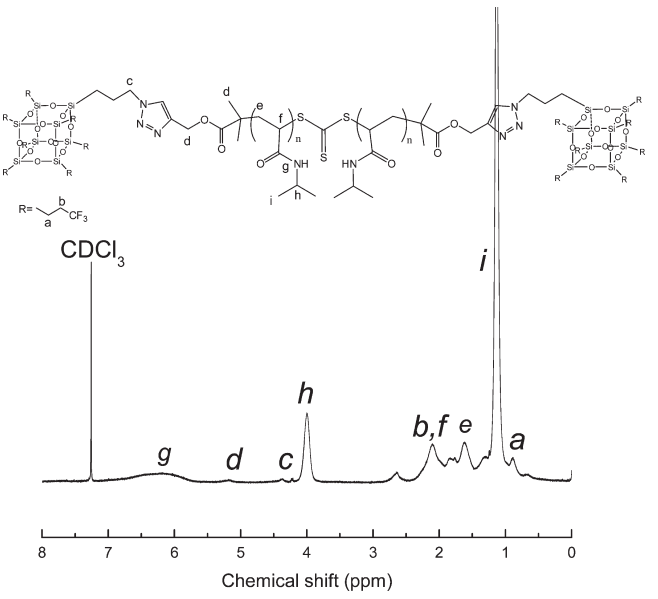

Figure 2. ^{1}H NMR spectrum of POSS-capped PNIPAAm with the length of PNIPAAm to be M_n = 8,700;.

protons of alkyne groups of BDPT indicates that all the terminal alkene groups of BDPT have totally reacted with the azido groups of POSS. With the occurrence of the click reaction, the resonance of the methylene proton connected to the azido groups completely shifted from 3.35 to 4.44 ppm, indicating that there are no unreacted POSS left. In terms of the ratio of integral intensity of methylne protons of POSS to methyl protons in the compound it is judged that POSS-capped trithiocarbonate (viz. bifunctional POSS CTA) was successuflly obtained.

The above POSS-capped trithiocarbonate was used as the chain transfer agent of NIPAAm and the RAFT polymerization was carried out with AIBN as the initiatior. For comparison, a plain PNIPAAm was synthesized with BDAT as the chain transfer agent. By controlling the molar ratios of the POSS-capped trithiocarbonate to NIPAAm and the conversions of the monomer, the POSS-capped PNIPAAm telechelics with variable lenghts of PNIPAAm were obtained. Representatively shown in Figure 2 is the ^{1}H NMR spectrum of POSS-capped PNIPAAm with the length of PNIPAAm to be M_n = 8700. Besides the proton resonance assignable to PNIPAAm chain, the new signals

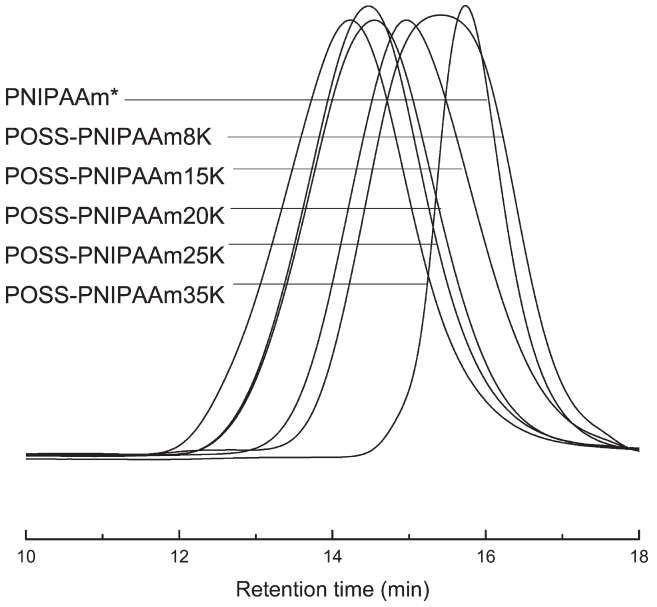

Figure 3. GPC curves of plain PNIPAAm and POSS-capped PNIPAAm telechelics. The plain PNIPAAm was prepared with BDAT as the chain transfer agent under the identical condition.

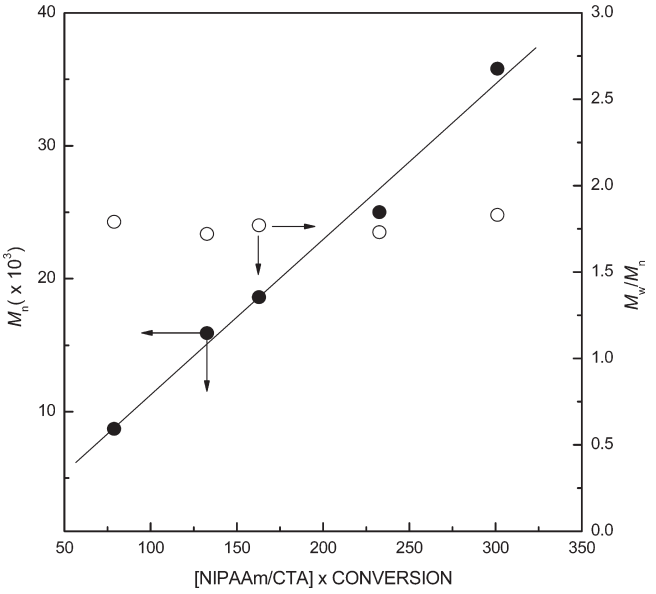

Figure 4. Plots of number-average molecular weights and polydispersity of molecular weight as functions of the product of the molar ratio of NIPAAm to the POSS-capped trithiocarbonate with conversion of NIPAAm.

Table 1. Results of Polymerization of NIPAAm with POSS-capped Trithiocarbonate As the Chain Transfer Agent

samples	[NIPAAm]/[CTA]	conversion of NIPAAm (wt%)	M_n	M_w/M_n
PNIPAAm*	126.4	81.4	12,400	1.26
POSS-PNIPAAm8K	88.3	89.2	8,700	1.79
POSS-PNIPAAm15K	176.7	75.0	15,900	1.72
POSS-PNIPAAm18K	235.6	69.1	18,600	1.77
POSS-PNIPAAm25K	340.6	68.3	25,000	1.73
POSS-PNIPAAm35K	474.9	63.4	35,800	1.83

* The plain PNIPAAm was synthesized with BDAT as the chain transfer agent under the identical condition.

of resonance were detected at 0.91 and 2.3 ppm, which was assignable to the protons of methylene groups connected to silicon atom and 3,3,3-trifluoromethyl groups of fluoropropyl group. This observation indicates that the resulting product combined the structural feature from PNIPAAm and POSS (see Scheme 2). All the POSS-capped PNIPAAm samples were subjected to gel permeation chromatography (GPC) to measure the molecular weights; the curves of GPC are presented in Figure 3 and the results of the RAFT polymerization are summarized in Table 1. It is seen that the GPC curves of all the POSS-capped PNIPAAm samples displayed unimodal peaks, implying that no unreacted POSS-terminated trithiocarbonate was detected during the polymerization. It is noted that the POSS-capped PNIPAAm possessed the polydispersity of molecular weights in the range of 1.72−1.82, irrespective of the length of PNIPAAm chain. The results of polymerization is in marked contrast to the case of the plain PNIPAAm with BDAT as the chain transfer agent with the polydispersity of M_w/M_n = 1.26. The broadened distribution of molecular weights could be responsible for the following factors: (i) the interactions of POSS and GPC column as evidenced by the observation that the broadening of GPC profile was pronounced while the content of POSS is high (e.g., POSS-PNIPAAm8K) and (ii) the use of the specific structure of the chain transfer agent. It is plausible to propose that there were the interactions between POSS and the packing of the GPC columns. For the RAFT polymerization with the POSS-capped trithiocarbonate as the chain transfer agent, the growth of PNIPAAm chain always occurred in the vicinity of the POSS end groups. It is plausible to propose that the low mobility and steric hindrance of the bulky POSS groups significantly affect the growth of chains. Nonetheless, the linear growth of PNIPAAm lengths as a function of the product of the molar ratio of POSS-terminated trithiocarbonate to NIPAAm with conversion of NIPAAm (see Figure 4) indicates that the polymerization of NIPAAm with the chain transfer agent was still in a living and controllable fashion. The results of ^{1}H NMR and GPC indicate that the POSS-capped PNIPAAm telechelics were successfully obtained.

Microphase Separation in POSS-capped PNIPAAm Telechelics. The morphology of the POSS-capped PNIPAAm telechelics was investigated by means of atomic force microscopy (AFM). The films of the samples were prepared via spin-coating technique. The surface AFM micrographs are presented in Figure 5. The left and right images are the topography and phase contrast images, respectively. It is noted that all the POSS-capped PNIPAAm telechelics displayed microphase-separated morphologies. In terms of the volume fraction of POSS and the difference in viscoelastic properties between PNIPAAm and POSS the light continuous regions are assignable to PNIPAAm matrix while the dark regions are attributed to the POSS domains. The spherical POSS domains with the size of 10−30 nm in diameter were dispersed into the continuous PNIPAAm matrix; the size of POSS domains decreased with increasing the length of PNIPAAm chains (or with decreasing the content of POSS). It is seen that besides some big POSS microdomains there were some smaller domains dispersed into the PNIPAAm matrix. This observation

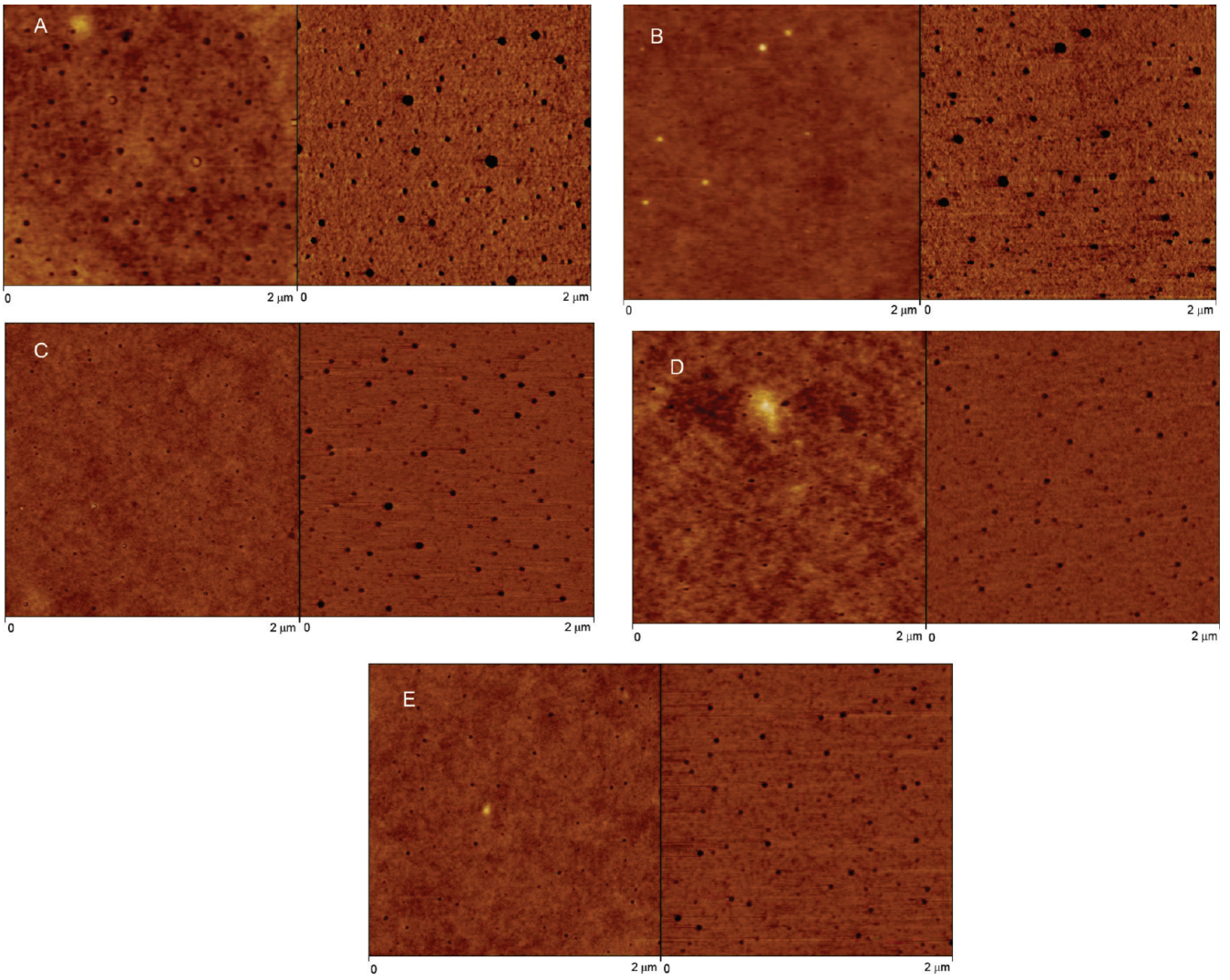

Figure 5. AFM micrographs: (A) POSS-PNIPAAm8K; (B) POSS-PNIPAAm15K; (C) POSS-PNIPAAm18 K; (D) POSS-PNIPAAm25K; (E) POSS-PNIPAAm35K. Left, height image; right, phase image.

could be associated with the degree of the migration of POSS components at the air−sample interfaces. The "big" microdomains are those that were migrated onto the interface between the samples and air. Because of the nature of low surface energy for organosilicon- and fluorine-containing component[24,63−70] the component of POSS will be enriched to the interface between the sample and air and thus the sizes of the POSS microdomains at the intimate surface of the films will be higher than those embedded into the matrix. It is plausible to propose that the smaller POSS domains are attributed to those POSS microdomains slightly below the surface of the samples.

Surface Wettability of POSS-capped PNIPAAm Telechelics. The enrichment of POSS component will significantly affect the water wettability of the sample surfaces, which can be examined by means of the measurement of static water contact angles. The surface contact angles (CA) were measured with water as the probe liquid. At room temperature (25 °C), the water contact angle of plain linear PNIPAAm was measured to be 49.1°, suggesting the hydrophilic nature of this polymer. It is of interest to note that the water contact angles of all the POSS-capped PNIPAAm telechelics were significantly higher than the plain PNIPAAm (See Figure 6). The contact angles enhanced with increasing the content of POSS. The enhanced contact angles suggest that the surface hydrophobicity of the films was significantly enhanced, i.e., the surface free energy was decreased.[71,72] The increased hydrophobicity for the surface of the POSS-capped PNIPAAm films is ascribed to the presence and enrichment of POSS component at the surface, which is in a good agreement with the results of morphological observation by the means of AFM.

Because of the thermoresponsive nature of PNIPAAm in aqueous solution, the temperature-dependent surface wettability of all the POSS-capped PNIPAAm films was investigated and the effect of POSS end groups on the surface hydrophobicity of PNIPAAm was examined. Prior to the CA measurement, the specimens were held at corresponding temperatures for 10 min. Shown in Figure 7 are the plots of water contact angles as functions of temperature for the plain PNIPAAm and the POSS-capped PNIPAAm telechelics. For the plain PNIPAAm, a sigmoid curve with a transition region in the vicinity of 32.8 °C was exhibited, which reflected the thermoresponsive properties of PNIPAAm in aqueous solution.[73−76] At the lower temperature (e.g., <32 °C) the water contact angles were lower than 50°, indicating that the surface was quite hydrophilic. The water contact angles increased with temperature with increasing the temperature,

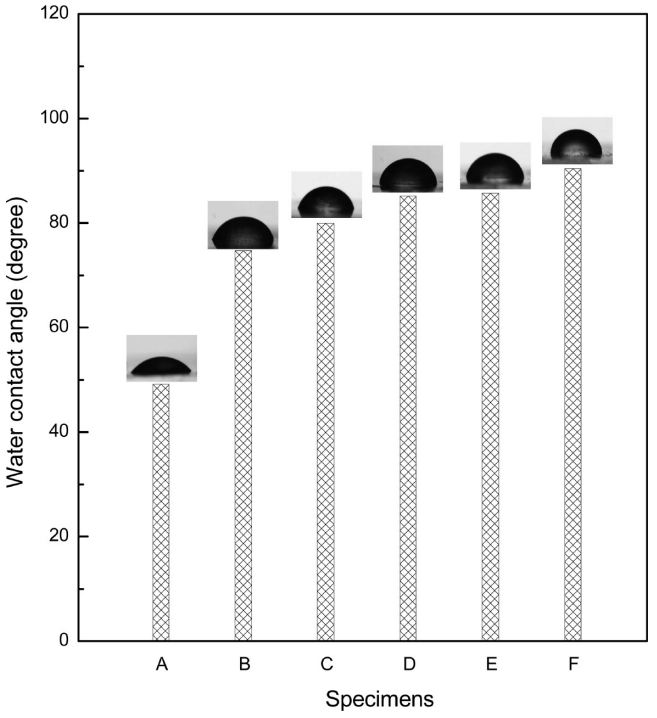

Figure 6. Plots of water contact angles for plain PNIPAAm and POSS-capped PNIPAAm telechelics at room temperature: (A) plain PNIPAAm; (B) POSS-PNIPAAm35K; (C) POSS-PNIPAAm25K; (D) POSS-PNIPAAm18K; (E) POSS-PNIPAAm15K; (F) POSS-PNIPAAm8K.

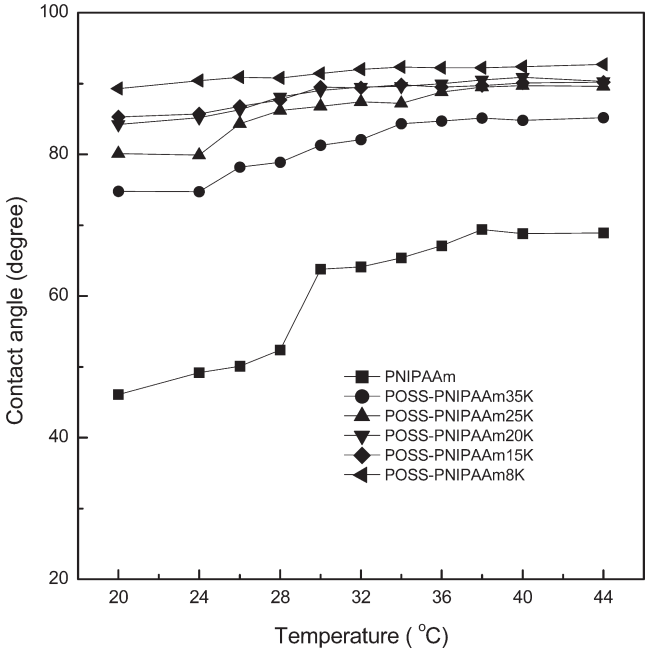

Figure 7. Plots of water contact angles as functions of temperature for plain PNIPAAm and POSS-capped PNIPAAm telechelics at room temperature.

suggesting that the surface became increasingly hydrophobic at elevated temperature (e.g., > 32 °C). The above phenomenon can be interpreted on the basis of the competition between intermolecular and intramolecular hydrogen bonding below

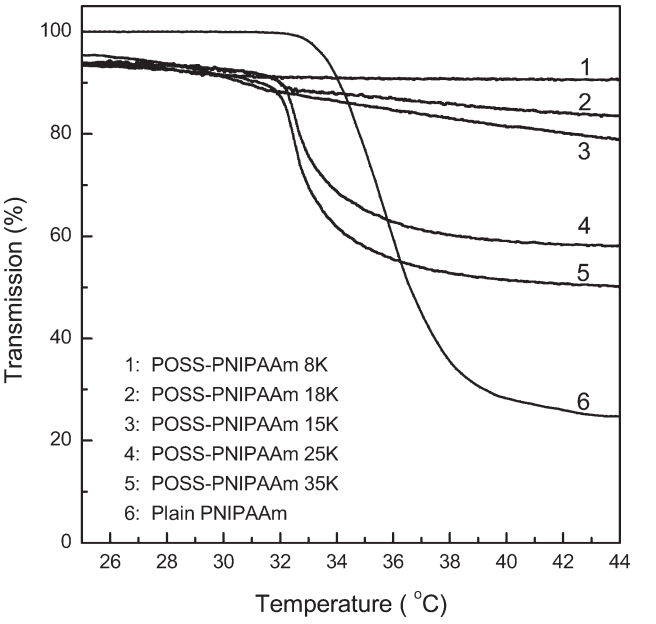

Figure 8. Plots of the transmission of the light (λ = 550 nm) as functions of temperature for the plain PNIPAAm and POSS-capped PNIPAAm solutions (0.02%) for the determination of LCSTs.

and above the lower critical solution temperature (LCST) of about 32 °C. Below the LCST, the intermolecular hydrogen bonding interactions between the PNIPAAm chains and water molecules results in the hydrophilicity of PNIPAAm film. Above the LCST, the intramolecular hydrogen bonding interactions between >C═O and N−H groups in the PNIPAAm chains are dominant, which gives rise to a compact and collapsed conformation of PNIPAAm chains and the surface of PNIPAAm became quite hydrophobic. For the POSS-capped PNIPAAm, the values of CAs were higher than that of plain PNIPAAm. The values of CA increased with increasing the percentage of POSS. For POSS-PNIPAAm8K, the CA at 25 °C was enhanced up to 90 °C, implying that the surface of the film was quite hydrophobic. It is noted that the enhancement in CA at the low temperature (<32 °C) is much more than at the elevated temperatures (>32 °C). As a consequence, the transition from hydrophilicity to hydrophobicity became increasingly feeble. This observation suggests that the effect of POSS enrichment at the surface on the hydrophilic surfaces is much more pronounced than on the hydrophobic surfaces.

Behavior of Hydrogels. *Lower Critical Solution Temperatures.* The low critical solution temperatures (LCST) of all the POSS-PNIPAAm telechelics were measured in views of the changes in the turbidity of the dilute aqueous solutions (0.2 wt %) as functions of temperature by means of UV−vis spectroscopy at a wavelength of λ = 550 nm. The plots of transmission of the light as functions of temperature are shown in Figure 8. It is seen that at the low temperatures all the POSS-capped PNIPAAm solutions had the transmission lower than that of the plain PNIPAAm solution. The decreased transmission could result from the formation of some aggregates of the self-organized nanoobjects of the POSS-capped PNIPAAm telechelics. It is seen that the transmission was decreased with increasing the temperature. The onsets of transmission reduction were taken as the LCST. The plot of LCST as a function of POSS percentage for the POSS-capped PNIPAAm telechelics is presented in Figure 9. Compared to plain PNIPAAm, the POSS-capped

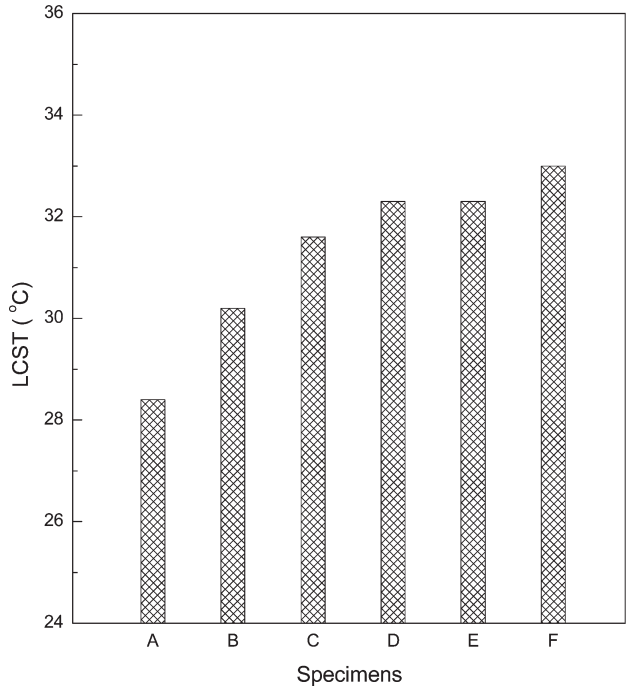

Figure 9. Plots of LCSTs for plain PNIPAAm and POSS-capped PNIPAAm telechelics: (A) POSS-PNIPAAm8K; (B) POSS-PNIPAAm15K; (C) POSS-PNIPAAm18K; (D) POSS-PNIPAAm25K; (E) POSS-PNIPAAm35K; and (F) plain PNIPAAm.

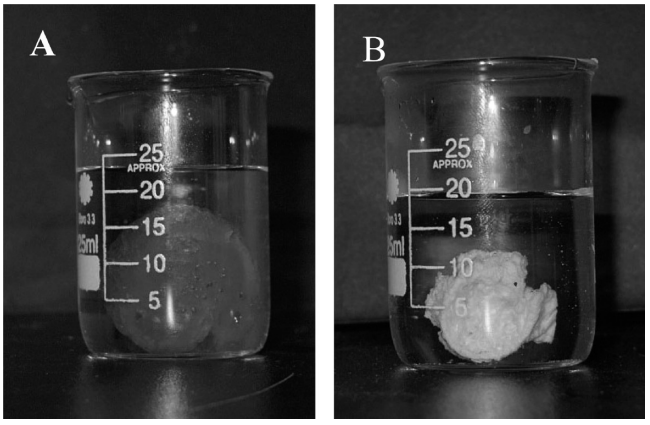

Figure 10. Photos of POSS-PNIPAAm18K physical hydrogel: at (A) 25 and (B) 45 °C.

PNIPAAm exhibited the depressed LCSTs. The LCST of POSS-PNIPAAm telechelics decreased with increasing the percentage of POSS end groups. The decreased LCST for the POSS-PNIPAAm telechelics is ascribed to the introduction of the hydrophobic component [viz. hepta(3,3,3-trifluoropropyl) POSS].

Behavior of Physical Hydrogels. All the POSS-capped PNIPAAm telechelics can be easily dissolved in commons solvents such as tetrahydrofuran and *N*,*N*′-dimethylformamide. However, they can only be swollen in water at room temperature as shown in Figure 10, indicating that the physical hydrogels were formed. The formation of physical hydrogels implies that there were some physically cross-linking sites in the hydrogels. It is proposed that the POSS microdomains constitute the physical cross-linking sites as evidenced by the results of AFM (see Figure 5). At room

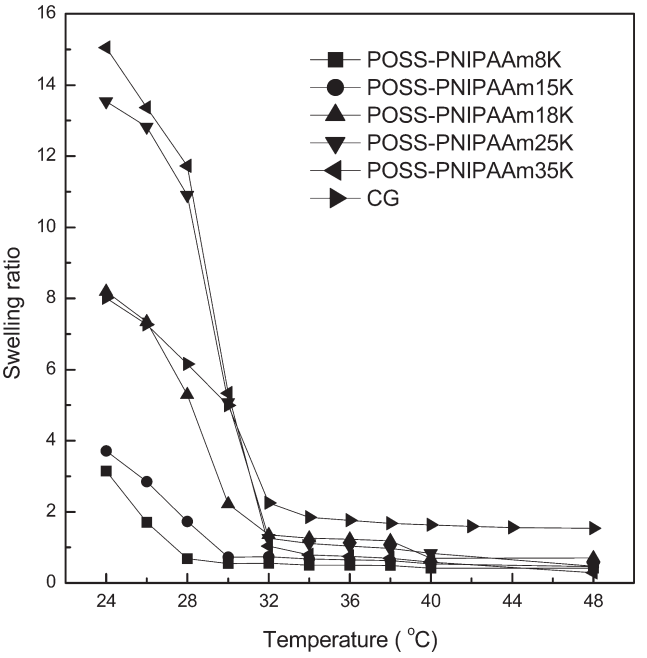

Figure 11. Plots of stable swelling ratio as functions of temperature for control PNIPAAm hydrogel (CG) and the POSS-capped PNIPAAm hydrogels.

temperature, the midblocks (i.e., PNIPAAm) were water-soluble whereas the end groups [viz. hepta(3,3,3-trifluoropropyl) POSS moiety] of the chains were highly hydrophobic and could be self-organized into the hydrophobic microdomains. These hydrophobic POSS microdomains would act as physical cross-linking sites connecting PNIPAAm chains and thus the physical hydrogels were afforded. At low temperature (e.g., < 30 °C), all the physical hydrogels were homogeneous and transparent. When heated up to the higher temperatures (e.g., > 40 °C), the hydrogels became shrank and the absorbed water was released, implying the occurrence of volume phase transition. When cooled, the hydrogels can be reswollen and become transparent again. The reversible swelling and deswelling behavior with temperature is characteristic of volume phase transition of PNIPAAm hydrogels. It is of interest to investigate the swelling, deswelling, and reswelling kinetics of the POSS-modified PNIPAAm physical hydrogels.

Shown in Figure 11 are the plots of swelling ratios as functions of temperature for the control PNIPAAm and the POSS-capped PNIPAAm hydrogels. In all the cases, the sigmoid curves of swelling ratio versus temperature were exhibited. It is noted that depending on the percentagte of POSS, the POSS-capped PNIPAAm hydrogels exhibited the temperatures of volume phase transtion (VPT) in the range of 28 to 32 °C. The VPT temperatures of the physicl hydrogels were identical with the LCSTs of the POSS-capped PNIPAAm telechilecs in water. It is noted that below the VPT temperatures the swelling ratios of POSS-PNIPAAm hydrogels increased with decreasing the percentage of POSS (or with increasing the length of PNIPAAm chains). The swelling ratios of the POSS-PNIPAAm8K and POSS-PNIPAAm15K hydrogels were much lower than that of the control PNIPAAm hydrogels. The POSS-PNIPAAm18K hydrogel possessed the swelling ratio quite close to that of the control hydrogels. It is seen that the swelling ratios of POSS-PNIPAAm25K and POSS-PINIPAAm35K even were much higher than that of the

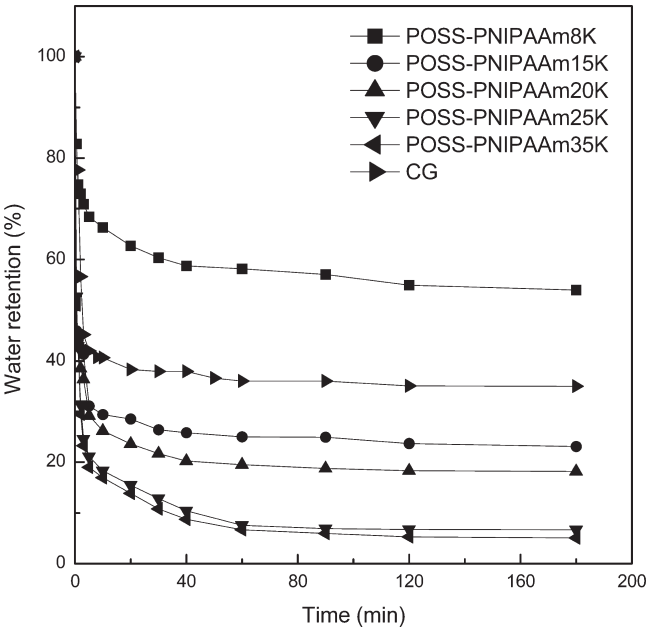

Figure 12. Plots of water retention as functions of deswelling time for evaluation of deswelling kinetics of CG and the POSS-capped PNIPAAm hydrogels.

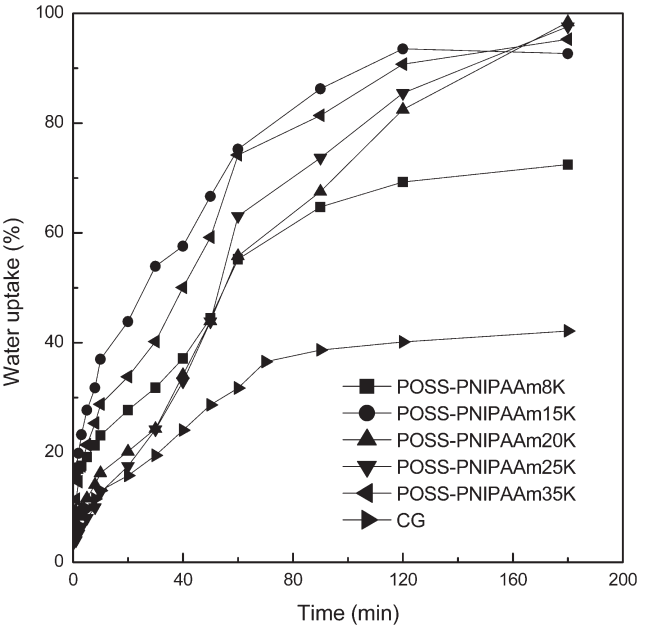

Figure 13. Plots of water uptake as functions of reswelling time for the measurement of reswelling kinetics of CG and the POSS-capped PNIPAAm hydrogels.

control PNIPAAm hydrogels. The dependence of swelling ratios on the percentage of POSS could be interpreted on the basis of the cross-linking densities of the physically cross-linked networks. For the control PNIPAAm hydrogel the swelling ratio was reduced from 8.0 to 1.60, i.e., 80 wt % absorbed water was released with the occurrence of volume phase transition. At elevated tmperatutres (>30 °C), all the POSS-capped PNIPAAm hydrogels displayed lower swelling ratios than the control PNIPAAm hydrogel. It is noted that the swelling ratios of all the POSS-capped PNIPAAm hydrogels were lower than 0.3, which was significantly lower than that (i.e., 1.6) of the control PNIPAAm hydrogels. For POSS-capped PNIPAAm8K, POSS-PNIPAAm15K, POSS-PNIPAAm18K, POSS-PNIPAAm25K, and POSS-PNIPAAm35K hydrogels 85.6, 86.4, 91.5, 95.9, and 97.7% of water absorbed in the hydrogels was released, respectively, with the occurrence of volume phase transtion. This observation suggests that under the identical condition the release of the abosrbed water for the POSS-capped PNIPAAm hydrogels was much faster than the control PNIPAAm hydrogel.

The deswelling behavior of the hydrogels was evaluated by measuring the swelling ratios of the hydrogels at 48 °C at variable times because the thermoresponsive hydrogels can shrink and release the absorbed water upon heating up to the VPT temperatures; the deswelling curves of the hydrogels are shown in Figure 12. It is of interest to note that the deswelling curves of all the POSS-PNIPAAm hydrogels were beneath that of the control PNIPAAm hydrogel. This observation indicates that under the identical condition the POSS-capped PNIPAAm hydrogels displayed much lower water retention than the control PNIPAAm hydrogel, i.e., upon deswelling, the POSS-modified hydrogels attained their stable water retention much faster than the control PNIPAAm hydrogel. For the control PNIPAAm hydrogel it takes ca. 10 min to attain the stable water retention of ca. 40.1%. However, within the identical time, the stable water retentions of the POSS-capped PNIPAAm hydrogels are lower than 29 wt % except for the POSS-PNIPAAm8K hydrogel. The water retention decreased with increasing the length of PNIPAAm chains. For instance, the stable water retention of POSS-PNIPAAm35K hydrogel was even as low as 16.3%. This result indicates that within the identical time, the POSS-PNIPAAm hydrogels are capable of releasing much more absorbed water than the plain hydrogel. The fact that POSS-PNIPAAm8K hydrogel displayed lower deswelling rate than other POSS-capped PNIPAAm hydrogels could be interpreted on the basis of the restriction of POSS microdomains on the change in macromolecular conformation of PNIPAAm chains from coils to globules due to too short PNIPAAm chains between the adjacent POSS microdomains. It is plausible to propose that the PNIPAAm chains at the intimate surfaces of POSS microdomains still remain quite hydrophiphilic even while the temperature was higher than the volume phase transition temperatures.[75]

To evaluate the reswelling behavior of the hydrogels, all the hydrogels were first deswelled at 48 °C in water and then the reswelling ratios were measured gravimetrically at 25 °C. Figure 13 shows the plots of water uptake as functions of time for the control and POSS-capped PNIPAAm hydrogels. It is noted that all the POSS-capped PNIPAAm hydrogels displayed the water uptake higher than the control hydrogels. For the control PNIPAM hydrogel, it takes 120 min to attain the water uptake of ca. 40 wt %. With the identical time, the swelling ratios of the modified hydrogels were significantly higher than this value, i.e., the reswelling rate of the POSS-PNIPAAm hydrogels was much higher than that of the control PNIPAAm hydrogel. It should be pointed out that the reswelling rates for the POSS-capped PNIPAAm hydrogels with the PNIPAAm length of 25 000 Da or higher could be subject to some overestimation since the shapes of these physical hydrogels were not well preserved after the long-time reswelling tests because of their too low cross-linking densities.

CONCLUSIONS

Hepta(3,3,3-trifluoropropyl) POSS-capped PNIPAAm telechelics with variable lengths of poly(N-isopropylacrylamide)

(PNIPAAm) were synthesized by the combination of reversible addition−fragmentation chain transfer polymerization (RAFT) and the copper-catalyzed Huisgen 1,3-cycloaddition. The organic−inorganic amphiphilic telechelics were characterized by means of nuclear magnetic resonance spectroscopy (NMR) and gel permeation chromatography (GPC). All the POSS-capped PNIPAAm telechelics exhibited various microphase-separated morphologies as evidenced by the morphological observation by means of atomic force microscopy (AFM). It is noted that the physical hydrogels were formed while these POSS-capped PNIPAAm telechelics were subjected to the solubility tests with water and the physical hydrogels possessed typical volume phase transition behavior as the temperatures were changed. The POSS-capped PNIPAAm hydrogels displayed rapid reswelling and deswelling thermoresponsive behavior compared to the control PNIPAAm.

AUTHOR INFORMATION

Corresponding Author

*Tel: 86-21-54743278. Fax: 86-21-54741297. E-mail: szheng@sjtu.edu.cn.

ACKNOWLEDGMENT

The financial support from Natural Science Foundation of China (20774058 and 50873059) and National Basic Research Program of China (2009CB930400) are acknowledged. The authors thank Shanghai Leading Academic Discipline Project (Project B202) for the partial support.

REFERENCES

(1) Schwab, J. J.; Lichtenhan, J. D. *Appl. Organomet. Chem.* **1998**, *12*, 707.
(2) Li, G.; Wang, L.; Ni, H.; Pittman, C. U. *J. Inorg. Organomet. Polym.* **2001**, *11*, 123.
(3) Abe, Y.; Gunji, T. *Prog. Polym. Sci.* **2004**, *29*, 149.
(4) Lin, W.-J.; Chen, W.-C.; Wu, W.-C.; Niu, Y.-H.; Jen, A.-K.-Y. *Macromolecules* **2004**, *37*, 2335.
(5) Pu, K.-Y.; Zhang, B.; Ma, Z.; Wang, P.; Qi, X.-Y.; Chen, R.-F.; Wuang, L.-H.; Fan, Q.-L.; Huang, W. *Polymer* **2006**, *47*, 1970.
(6) Miyake, J.; Chujo, Y. *Macromol. Rapid Commun.* **2008**, *29*, 86.
(7) Bandi, S.; Bell, M.; Schiraldi, D. A. *Macromolecules* **2005**, *38*, 9216.
(8) Mu, J.; Zheng, S. *J. Colloid Interface Sci.* **2007**, *307*, 377.
(9) Zeng, K.; Fang, Y.; Zheng, S. *J. Polym. Sci., Part B: Polym. Phys.* **2009**, *47*, 504.
(10) Zeng, K.; Wang, L.; Zheng, S. *J. Phys. Chem. B* **2009**, *113*, 11831.
(11) Wright, M. E.; Petteys, B. J.; Guenthner, A. J.; Fallis, S.; Yandek, G. R.; Tomczak, S. J.; Minton, T. K.; Brunsvold, A. *Macromolecules* **2006**, *39*, 4710.
(12) Hao, N.; Boehning, M.; Schoenhals, A. *Macromolecules* **2007**, *40*, 9672.
(13) Chou, C.-H.; Hsu, S.-L.; Yeh, S.-W.; Wang, H.-S.; Wei, K.-H. *Macromolecules* **2005**, *38*, 9117.
(14) Kang, J.-M.; Cho, H.-J.; Lee, J.; Lee, J.-I.; Lee, S.-K.; Cho, N.-S.; Hwang, D.-H.; Shi, H.-K. *Macromolecules* **2006**, *39*, 4999.
(15) Knight, P. T.; Lee, K. M.; Chung, T.; Mather, P. T. *Macromolecules* **2009**, *42*, 6596.
(16) Normatov, J.; Silverstein, M. S. *Macromolecules* **2007**, *40*, 8329.
(17) Lee, J.; Cho, H.-J.; Jung, B.-J.; Cho, N. S.; Shim, H.-K. *Macromolecules* **2004**, *37*, 8523.
(18) Chou, C.-H.; Hsu, S.-L.; Dinakaran, K.; Chiu, M.-Y.; Wei, K.-H. *Macromolecules* **2005**, *38*, 745.
(19) Lee, W.; Ni, S.; Deng, J.; Kim, B.-S.; Satija, S. K.; Mather, P. T.; Esker, A. R. *Macromolecules* **2007**, *40*, 682.
(20) Yuan, H.; Luo, K.; Lai, Y.; Pu, Y.; He, B.; Wang, G.; Wu, Y.; Gu, Z. *Mol. Pharm.* **2010**, *7*, 4953.
(21) Yang, X.; Froehlich, J. D.; Chae, H. S.; Harding, B. T.; Li, S.; Mochizuki, A.; Jabbour, G. E. *Chem. Mater.* **2010**, *22*, 4776.
(22) Chhatre, S. S.; Guardado, J. O.; Moore, B. M.; Haddad, M. S.; Mabry, J. M.; McKinley, G. H.; Cohen, R. E. *ACS Appl. Mater. Interfaces* **2010**, *2*, 3544.
(23) Decker, B.; Hartmann-Thompson, C.; Carver, P. I.; Keinath, S. E.; Santurri, P. R. *Chem. Mater.* **2010**, *22*, 942.
(24) Wu, J.; Hou, S.; Ren, D.; Mather, P. T. *Biomacromolecules* **2009**, *10*, 2686.
(25) Kikuchi, A.; Okano, T. *Prog. Polym. Sci.* **2002**, *27*, 1165.
(26) Gil, E. S.; Hudson, S. M. *Prog. Polym. Sci.* **2004**, *29*, 1173.
(27) Hoare, T.; Pelton, R. *Macromolecules* **2007**, *40*, 670.
(28) Zhang, X.-Z.; Xu, X.-D.; Cheng, S.-X.; Zhuo, R.-X. *Soft Matter* **2008**, *4*, 385.
(29) Hirokawa, Y.; Tanaka, Y. *J. Chem. Phys.* **1984**, *81*, 6379.
(30) Matsuo, E. S.; Tanaka, T. *J. Chem. Phys.* **1988**, *89*, 1695.
(31) Suzuki, A.; Tanaka, T. *Nature* **1990**, *346*, 345.
(32) Otake, K.; Inomata, H.; Konno, M.; Saito, S. *Macromolecules* **1990**, *23*, 283.
(33) Inomata, H.; Goto, S.; Otake, K.; Saito, S. *Langmuir* **1992**, *8*, 687.
(34) Shibayama, M.; Morimoto, M.; Nomura, S. *Macromolecules* **1994**, *27*, 5060.
(35) Liang, L.; Rieke, P. C.; Liu, J.; Fryxell, G. E.; Young, J. S.; Engelhard, M. H.; Alford, K. L. *Langmuir* **2000**, *16*, 8016.
(36) Yin, X.; Hoffman, A. S.; Stayton, P. S. *Biomacromolecules* **2006**, *7*, 1381.
(37) Heskins, M.; Guillet, J. E.; James, E. *J. Macromol. Sci. Chem* **1968**, *A2*, 1441.
(38) Kujawa, P.; Tanaka, F.; Winnik, F. M. *Macromolecules* **2006**, *39*, 3048.
(39) Schild, H. G. *Prog. Polym. Sci.* **1992**, *17*, 163.
(40) Wu, C. *Macromolecules* **1997**, *30*, 574.
(41) Kujawa, P.; Winnik, F. M. *Macromolecules* **2001**, *34*, 4130.
(42) Takigawa, T.; Araki, H.; Takahashi, K.; Masuda, T. *J. Chem. Phys.* **2000**, *113*, 7640.
(43) Haraguchi, K.; Farnworth, R.; Ohbayashi, A.; Takehisa, T. *Macromolecules* **2003**, *36*, 5732.
(44) Nakamoto, C.; Motonaga, T.; Shibayama, M. *Macromolecules* **2001**, *34*, 911.
(45) Yoshida, R.; Uchida, K.; Kaneko, Y.; Sakai, K.; Kikuchi, A.; Sakurai, Y.; Okano, T. *Nature (London)* **1995**, *374*, 240.
(46) Haraguchi, K.; Takehisa, T. *Adv. Mater.* **2002**, *14*, 1120.
(47) Kim, B. S.; Mather, P. T. *Macromolecules* **2002**, *35*, 8378.
(48) Kim, B. S.; Mather, P. T. *Macromolecules* **2006**, *39*, 9253.
(49) Kim, B. S.; Mather, P. T. *Polymer* **2006**, *47*, 6202.
(50) Zhang, W.; Mueller, A.H. E. *Macromolecules* **2010**, *43*, 3148.
(51) Zeng, K.; Wang, L.; Zheng, S.; Qian, X. *Polymer* **2009**, *50*, 685.
(52) Turri, S.; Levi, M. *Macromolecules* **2005**, *38*, 5569.
(53) Liu, F.; Tao, G. L.; Zhuo, R.-X. *Polymer J.* **1993**, *25*, 561.
(54) Koh, K.; Sugiyama, S.; Morinaga, T.; Ohno, K.; Tsujii, Y.; Fukuda, T.; Yamahiro, M.; Iijima, T.; Oikawa, H.; Watanabe, K.; Miyashita, T. *Macromolecules* **2005**, *38*, 1264.
(55) Lai, J. T.; Filla, D.; Shea, R. *Macromolecules* **2002**, *35*, 6754.
(56) Bouchekif, H.; Narain, R. *J. Phys. Chem. B* **2007**, *111*, 11120.
(57) Nuopponen, M.; Ki, K. K.; Laukkanen, A.; Hietala, S.; Tenhu, H. *J. Polym. Sci., Part A: Polym. Chem.* **2008**, *46*, 38.
(58) Kirkland, S. E.; Hensarling, R. M.; Mcconaughy, S. D.; Guo, Y.; Jarrett, W. L.; Mccormick, C. L. *Biomacromolecules* **2008**, *9*, 481.
(59) Jia, Z.; Xu, X.; Fu, Q.; Huang, J. *J. Polym. Sci., Part A: Polym. Chem.* **2006**, *44*, 6071.
(60) Ranjan, R.; Brittain, W. J. *Macromolecules* **2007**, *40*, 6217.
(61) Lian, X.; Jin, J.; Tian, J.; Zhao, H. *ACS Appl. Mater. & Interface* **2010**, *2*, 2261.

(62) Wu, D.; Song, X.; Tang, T.; Zhao, H. J. *Polym. Sci.: Part A: Polym. Chem.* **2010**, *48*, 443.
(63) Zeng, K.; Zheng, S. *Macromol. Chem. Phys.* **2009**, *210*, 783.
(64) Feast, W. J.; Munro, H. S.; Richarsa, R. W., Eds. *Polymer Surface and Interface II*; John Wiley & Sons: Chichester, U.K., 1993.
(65) Affrossman, S.; Bertrand, R.; Hartshorne, M.; Kiff, T.; Leonard, D.; Pethrick, R. W. *Macromolecules* **1996**, *29*, 5432.
(66) Youngblood, J. P.; McCarthy, T. J. *Macromolecules* **1999**, *32*, 6800.
(67) Li, X. F.; Chiellini, E.; Galli, G.; Ober, C. K.; Hexemer, A.; Kramer, E. J.; Fisher, D. A. *Macromolecules* **2002**, *35*, 8078.
(68) Hirao, A.; Koide, G.; Sugiyama, K. *Macromolecules* **2002**, *35*, 7642.
(69) O'Rourke-Muisener, P. A. V.; Jalbert, C. A.; Yuan, C.; Baezold, J.; Mason, R.; Wong, D.; Kim, Y. J.; Koberstein, J. D.; Gunesin, B. *Macromolecules* **2003**, *36*, 2956.
(70) Koberstein, J. T. *J. Polym. Sci., Part B: Polym. Phys.* **2004**, *42*, 2942.
(71) Mabry, J. M.; Vij, A.; Iacono, S. T.; Viers, B. D. *Angew. Chem., Int. Ed.* **2008**, *47*, 4137.
(72) Iacono, S. T.; Vij, A.; Grabow, W.; Smith, D. W.; Mabry, J. M. *Chem. Comm* **2007**, 4992.
(73) Zhang, J.; Pelton, R.; Deng, Y. *Langmuir* **1995**, *11*, 2301.
(74) Liang, L.; Rieke, P. C.; Liu, J.; Fryxell, G. E.; Young, J. S.; Engelhard, M. H.; Alford, K. L. *Langmuir* **2000**, *16*, 8016.
(75) Turan, E.; Demirci, S.; Caykara, T. *Thin Solid Films* **2010**, *518*, 5950.
(76) Pelton, R. *J. Colloid Interface Sci.* **2010**, *348*, 673.